frontiers | Frontiers in Forests and Global Change

TYPE Original Research
PUBLISHED 30 April 2025
DOI 10.3389/ffgc.2025.1572414

OPEN ACCESS

EDITED BY
Jiquan Chen,
Michigan State University, United States

REVIEWED BY
Hang Xu,
Beijing Forestry University, China
Lixin Wang,
Indiana University Indianapolis, United States

*CORRESPONDENCE
Xiaowei Zhao
✉ xwzever@163.com

RECEIVED 07 February 2025
ACCEPTED 07 April 2025
PUBLISHED 30 April 2025

CITATION
Zhao X and Zhu L (2025) Sensitivity of transpiration to influencing factors at varying drought levels in *Schima superba*.
Front. For. Glob. Change 8:1572414.
doi: 10.3389/ffgc.2025.1572414

Sensitivity of transpiration to influencing factors at varying drought levels in *Schima superba*

Xiaowei Zhao[1]* and Liwei Zhu[2]

[1]School of Urban and Rural Planning and Architectural Engineering, Shangluo University, Shangluo, China, [2]Key Laboratory of Vegetation Restoration and Management of Degraded Ecosystems, Guangdong Provincial Key Laboratory of Applied Botany, South China Botanical Garden, Chinese Academy of Sciences, Guangzhou, China

Introduction: Uneven rainfall distribution alters tree water use patterns, ultimately influencing plantation establishment.

Methods: Based on monthly rainfall, six drought levels were classified. Whole-tree sap flux and meteorological variables were monitored across these levels from 2010 to 2013 in a pure *Schima superba* plantation in South China. The relationships between daily transpiration (T_t) and the influencing factors were modeled using the Support vector regression (SVR) method. Shapley additive explanations (SHAP) values were employed to characterize the sensitivity and contributions of four environmental variables to T_t.

Results: The results indicate that monthly rainfall (RF_t) significantly influences the sensitivity of these four environmental variables to T_t when RF_t exceeds 300 mm (Level 6). Furthermore, when RF_t is 300 mm or less (Levels 1–5), the sensitivity of these factors and their total contributions to T_t are independent of tree size.

Discussion: Our findings indicate that the decoupling between T_t and environmental factors may be a significant characteristic of ongoing water stress during high rainfall months. Additionally, these findings enhance the predictive capability of machine learning models in assessing tree water use.

KEYWORDS

transpiration, white noise, SHAP values, support vector regression, time series

Introduction

Global climate change has led to an increase in the number of extreme weather events in recent years (Zia et al., 2021; Brunet et al., 2024). Since the year 2000, southern China has experienced several severe droughts, particularly during four significant events in 2001, 2006–2007, 2009–2010 and 2020–2021, which have been identified as extreme "Water crisis" (Zhang et al., 2018). The uneven distribution of rainfall is a major factor contributing to drought in this region, which seriously affects the ecological establishment of plantations. Specifically, the intensity and frequency of rainfall profoundly influence the physiological behavior and ecological environment of trees. Even during prolonged mild to moderate drought, trees become particularly vulnerable to carbon starvation and biological invasion, potentially leading to chronic mortality (McDowell et al., 2008; da Silva et al., 2013; Anderegg et al., 2013; Chen et al., 2018; Kono et al., 2019).

Transpiration plays a crucial role in the physiological functioning of trees and serves as the primary mechanism for water use. Its dynamics are influenced by various internal and external factors. Meteorological conditions primarily govern instantaneous changes in transpiration, while soil factors determine its overall level (Wullschleger et al., 1998; Jiao et al., 2019). However, these influences may differ among trees of various sizes and ontogenetic stages (Andrade et al., 1998; Meinzer et al., 2001; Meinzer, 2003). Long-term synchronous monitoring of whole-tree sap flow and environmental factors significantly enhance our understanding of the relationship between these internal and external factors influencing tree water use, ultimately improving prediction efficiency. However, few studies have focused on the performance of tree transpiration responses to meteorological factors under varying drought conditions.

Environmental factors are critical in driving water movement within plants. Photosynthetically active radiation (PAR_t) influences the opening and closing of stomata by affecting the amount of CO_2 absorbed during photosynthesis and heating the leaf surface, which subsequently impacts transpiration rates (Kume, 2017; Li et al., 2021). The air vapor pressure deficit (VPD_t) significantly alters the water vapor pressure difference between the leaves and the surrounding air, directly affecting the transport of water vapor from the internal leaf to the external atmosphere (Fricke, 2017). Similarly, wind speed (WS_t) affects the boundary layer resistance of plant leaves, as well as the dynamics of stomatal opening and closing and overall leaf temperature (Monteith and Mike, 1990; Holwerda et al., 2012; Carvalho et al., 2015). Furthermore, soil moisture content (SM_t) impacts the ability of plant roots to absorb and transport water. A thorough understanding of these causal relationships provides a theoretical basis for predicting transpiration models based on environmental factors (Jarvis, 1976). The close relationships between sap flow, transpiration calculated based on sap flow and environmental factors have been demonstrated using double-variable analysis and multiple linear regression in different climate zones and forest types (e.g., Juhász et al., 2013; Shen et al., 2015; Wang et al., 2017; Han et al., 2019; Chen et al., 2022). However, multiple linear regression requires strict null assumptions, including linearity, independence and normality, while double-variable analysis did not adequately quantify the contributions of eigenvalues. In contrast, machine learning (ML) methods does not impose these stringent requirements. They not only demonstrate higher prediction accuracy and stability in drought sensitivity analysis but also effectively uncover and capture the relationships between input variables and forecast outcomes. Furthermore, they elucidates interactions among input variables through interpretive tools such as the SHAP algorithm and more sophisticated models. This comprehensive approach enhances our understanding of which factors are most sensitive to drought prediction (Zhang et al., 2024; Uexkull et al., 2016; Saha et al., 2023). Although ANNs are gaining increasingly popularity in predicting tree transpiration due to their flexible requirements (e.g., Liu et al., 2009; Whitley et al., 2009; Xu et al., 2017; Tu et al., 2019), there are currently no studies on Support vector Regression (SVR) in this context. The study emphasizes exploring the application of ML methods for analyzing tree transpiration sensitivity to drought. The objectives of this paper are to (1) determine the sensitivity of meteorological factors to the transpiration of three tree sizes across six levels of drought, as well as their total contributions to transpiration using SVR, and (2) examine how these responses vary with different drought levels and tree sizes.

Materials and methods

Field site and plant materials

The experiments were conducted at the South China Botanical Garden station of the Chinese Academy of Sciences in Guangzhou, Guangdong, China (113°21′E，23°10′N, 40 m altitude). This area experiences a subtropical monsoon climate, characterized by a wet season (April to September) and a dry season (November to January), with an annual average temperature of 21.8°C. The region receives an averages annual precipitation in 1710.5 mm, with over 80% occurring during the wet season. A pure *Schima superba* forest was established in the mid-1980s at a density of 1,046 plants per hectare. We sampled 15 30-year-old individuals as test objects and divided them into three size classes based on the method of Mei et al. (2010a) (Table 1).

Sap flux density and transpiration measurement

Granier's thermal dissipation probe (TDP) (Granier, 1985) was used to measure xylem sap flux density (F_t , g·m^{-2}·s^{-1}). These probes were 2 mm in diameter and 20 mm in length, consisting of a copper-constantan thermojunction. They were radially inserted into the sapwood of the stem samples at approximately 0.15 m apart vertically at breast height. The sensors were placed on the northern side and covered with aluminum foil to protect them from sunlight, while the top of the probes was sealed with waterproof silicone. The heated upper probe was supplied with a constant power of 0.2 W, while the unheated lower probe served as a reference. The temperature difference between the two probes were averaged every 30 s, and data were collected at 10-min intervals using a Delta-T logger. These records were then used to calculate F_t using the empirical equation proposed by Granier (1987). Due to the substantial variation in sap flux at depths greater than 40 mm in the sapwood of *Schima Superba* (approximately 45% of the flux occurs at depths of 0-40 mm) (Mei et al., 2010b), the mean flux was calculated by adding the sap flux at these two depths, weighted by their respective areas. The weights were determined based on the ratio of sapwood area within the two depths to the total sapwood area. Whole-tree transpiration (T_t , g) was calculated every 10 min by

$$T_t = \sum\left(F_{0-40} \times A_{0-40} + F_{40} \times A_{40}\right) \times \mathrm{t} \tag{1}$$

where, F_{0-40} and F_{40} represent the sap flux density in the outer xylem (0–40 mm) and inner xylem (>40 mm), respectively, while A_{0-40} and A_{40} are the sapwood areas corresponding to these densities, as calculated by Zhao et al. (2018). The time interval, t, is 600 s, with data averaged and recorded every 10 min by the logger.

Environmental measurements

Five environmental variables were monitored approximately 2 m above the forest upper canopy. Wind speed (WS_t , m·s^{-1}) was monitored using an AN4 Anemometer (Delta-T Devices Ltd., Cambridge, UK). Air temperature (Ta , °C) and relative humidity (RH , %) were monitored using a RHT2V-418 sensor (Delta-T Devices Ltd., Cambridge, UK). The air vapor pressure deficit (VPD_t , kPa) was calculated using the difference in vapor pressure between saturated and ambient air, combining the effects of air temperature and relative humidity. Photosynthetically active radiation (PAR_t , W·m^{-2}) was monitored with a Li-Cor quantum sensor (LI-190SA, LI-COR, USA). Soil moisture content (SM_t , m^{-3}·m^{-3}) was assessed using three frequency domain sensors (SM200, Delta-T Devices, UK) at a depth of 30–40 cm. Monthly rainfall (RF_t , mm) data were

TABLE 1 Characteristics of tree samples.

Tree class	Tree no.	DBH (m)	Height (m)	Crown diameter (m^2)	Bark thickness at DBH (m)	Sapwood Area (m^2)	Sapwood Area at depth of 0-40 mm (m^2)
Class 1	Tree 1	0.151	15.3	14.7	0.40	0.0688	0.0382
	Tree 2	0.194	12.6	28.8	0.75	0.113	0.0523
	Tree 4	0.220	15.3	6.6	0.90	0.146	0.0609
	Tree 5	0.224	15.5	6.9	0.70	0.151	0.0622
	Tree 10	0.240	16.9	7.0	0.80	0.174	0.0674
	Mean	0.197	15.1	12.8	0.71	0.117	0.0534
Class 2	Tree 3	0.133	12.1	4.5	0.45	0.0534	0.0322
	Tree 6	0.095	11.0	1.2	0.35	0.0273	0.0197
	Tree 7	0.175	12.9	5.5	0.7	0.0924	0.0461
	Tree 11	0.135	11.2	2.9	0.45	0.055	0.0329
	Tree 13	0.084	12.0	3.1	0.35	0.0214	0.0161
	Tree 14	0.144	13.1	4.4	0.55	0.0626	0.0359
	Mean	0.128	12.1	3.6	0.45	0.0544	0.0326
Class 3	Tree 8	0.088	9.7	3.4	0.40	0.0234	0.0174
	Tree 9	0.088	9.5	2.3	0.35	0.0234	0.0174
	Tree 12	0.065	8.0	2.0	0.30	0.0128	0.00988
	Tree 15	0.073	9.7	2.4	0.25	0.0161	0.0125
	Mean	0.079	9.2	2.5	0.33	0.0234	0.0174

DBH, Diameter at breast height (1.3 m).

obtained from the Guangzhou Statistics Bureau[1]. All variables were recorded using the same logger as the sap flux measurements.

SVR

Support vector regression (SVR) is a significant extension of Support vector machine (SVM) specifically designed to address regression problems. It works by identifying a hyperplane defined by the equation $f(x) = \omega^T x + b$ (representing the predicted value in the linear case) that creates a margin of $\left[f(x) - \varepsilon, f(x) + \varepsilon\right]$. The goal is to position this hyperplane so that most training samples fall within the margin, satisfying the condition $|y - f(x)| \leq \varepsilon$, while keeping the complexity of the model as low as possible. This process can be formulated as an optimization problem:

$$\min \frac{1}{2}\|\omega\|^2 + C\sum_{i=1}^{m}\left(\xi_i + \xi_i^*\right) \tag{2}$$

$$\text{subject to} \begin{cases} y_i - \omega^T x_i - b \leq \varepsilon + \xi_i \\ \omega^T x_i + b - y_i \leq \varepsilon + \xi_i^* \\ \xi_i, \xi_i^* \geq 0, i = 1, \ldots, m. \end{cases}$$

where ω denotes the weight vector, $C > 0$ is the regularization parameter that balances the model's fit accuracy and generalization ability (with $C = 0.08$ here). ε is the tolerance for prediction error (with ε =0.01 here). These two parameters can be determined using GridSearchCV from Scikit-learn. b is the bias, x_i is the i-th observation of the input vector ($x \in R^d$), and ξ_i and ξ_i^* are slack variables for guarding against outliers.

To transform the constrained optimization problem (Equation 2) into an unconstrained optimization one, Lagrange multipliers are introduced to formulate the Lagrangian function:

$$\begin{aligned} L\left(\omega, \xi^*, \xi, \lambda, \lambda^*, \alpha, \alpha^*\right) &= \frac{1}{2}\|\omega\|^2 + C\sum_{i=1}^{m}\left(\xi_i + \xi_i^*\right) \\ &+ \sum_{i=1}^{m}\alpha_i\left(-y_i + \omega^T x_i + b - \varepsilon - \xi_i\right) \\ &+ \sum_{i=1}^{m}\alpha_i^*\left(y_i - \omega^T x_i - b - \varepsilon - \xi_i^*\right) - \sum_{i=1}^{m}\lambda_i\xi_i + \lambda_i^*\xi_i^* \end{aligned} \tag{3}$$

Where α_i, α_i^*, λ_i and λ_i^* are Lagrange multipliers; the first two correspond to inequality constraints, while the last two are associated with the non-negative constraints.

The minimum of Equation 3 can be determined based on the Karush-Kuhn-Tucker (KKT) conditions, yielding the dual optimization form in Equation 4 by taking the partial derivatives with respect to ω, b, ξ_i and ξ_i^* (Vapnik, 1995; Smola and Schölkopf, 2004):

$$\begin{aligned} \max -\frac{1}{2}\sum_{i,j=1}^{m}\left(\alpha_i - \alpha_i^*\right)\left(\alpha_j - \alpha_j^*\right)x_i x_j - \varepsilon\sum_{i=1}^{m}\left(\alpha_i + \alpha_i^*\right) \\ + \sum_{i=1}^{m}y_i\left(\alpha_i - \alpha_i^*\right) \end{aligned} \tag{4}$$

1 http://tjj.gz.gov.cn/

$$\text{subject to} \begin{cases} \sum_{i=1}^{m}\left(\alpha_i^* - \alpha_i\right) = 0 \\ 0 \le \alpha_i, \alpha_i^* \le C \end{cases}$$

thus, ω is equal to $\sum_{i=1}^{m}\left(\alpha_i^* - \alpha_i\right)x_i$, and the function approximation can be rewritten as follows:

$$f(x) = \sum_{i=1}^{m}\left(\alpha_i^* - \alpha_i\right)x + b \tag{5}$$

Equation 5 represents the linear case (Kernel = 'Linear'). For the nonlinear case, SVR can map the input data to a higher-dimensional kernel space using kernel functions such as Gaussian, Polynomial and Sigmoid kernels.

Data and analyses

According to the Chinese meteorological industry standard 'Rainfall Process Classification' (QX/T 489–2019), six levels of rainfall intensity were defined based on monthly rainfall to explore the sensitivity of environmental factors to sap flux in three classes of *S. superba* under drought stress (Table 2). Accordingly, six datasets were selected from the years 2010–2013, each comprising 10-min interval sap flux data and the corresponding environmental data when PAR_t was at least 5 w·m^{-2}. Of these datasets, 80% were used for training, while the remaining 20% were used for testing. Daily transpiration (T_t), calculated using Equation 1 for each class, was modeled as an output series using SVR with Scikit-learn in Python 3.12, with environmental variables served as input series. All series were standardized, denoised, and made stationary using the z-score method, Haar transformation, and differencing before modeling. Their stationarity and white noise characteristics were assessed using the Augmented Dickey-Fuller test and the Portmanteau test. During the testing phase, the Nash-Sutcliffe Efficiency coefficient (NSE) and Root Mean Square Error based on the observations' standard deviation (RSR) were used to evaluate the effectiveness of the SVM models considering their advantages (Moriasi et al., 2007). The Root Mean Square Error (RMSE) was utilized to determine the optimum kernel function.

$$\text{NSE} = 1 - \frac{\sum_{i=1}^{n}\left(P_i - O_i\right)^2}{\sum_{i=1}^{n}\left(O_i - \bar{O}_i\right)^2} \tag{6}$$

$$\text{RSR} = \sqrt{\frac{\sum_{i=1}^{n}\left(P_i - O_i\right)^2}{\sum_{i=1}^{n}\left(O_i - \bar{O}_i\right)^2}} \tag{7}$$

$$\text{RMSE} = \sqrt{\frac{\sum_{i=1}^{n}\left(O_i - \bar{O}_i\right)^2}{n}} \tag{8}$$

Where P_i is the predicted value, O_i is the actual value, and $\bar{O}_i$ is the average of the actual value; n is the total number of datasets. The prediction accuracy of the models was evaluated as follows: I. very good ($0.75 < \text{NSE} \le 1$ and $0 \le \text{RSR} \le 0.5$); II. good ($0.65 < \text{NSE} \le 0.75$ and $0.5 < \text{RSR} \le 0.6$); III. Satisfactory ($0.5 < \text{NSE} \le 0.65$ and $0.6 < \text{RSR} \le 0.7$); IV. unsatisfactory ($\text{NSE} \le 0.5$ and $0.7 < \text{RSR}$).

Shapley additive explanations (SHAP) was first utilized to explain the results of the SVR models for T_t. Unlike traditional correlation and determination coefficients, SHAP values can highlight the direction of each feature's contribution and quantify their impacts on the final prediction, regardless of whether they are present in the test instances (Mastropietro et al., 2023). In this context, the sensitivity of environmental factors to T_t is quantified by the mean value of |SHAP|. A higher mean value indicates greater sensitivity of those factors to T_t, and vice versa. The accumulation of SHAP values reflects the total contributions of these factors to T_t.

Results

Daily transpiration, sap flux and environmental factors variation

At all six levels, the coefficient of variation (CV.) of T_t and F_t exhibited consistent variation (Figure 1a), while their means did not align (Figure 1b). The T_t of Class 1 was the highest, followed by Class 2 and 3. In contrast, F_t did not consistently follow the class order, with the exception of Level 2, where Class 2 showed the highest value. This suggests that larger trees use more water in terms of transpiration. Notably, both

TABLE 2 Characteristics of six levels and data choosing.

Drought	Month rainfall (mm)	Days	Daily interval (UTC + 8)	Observations
Level 1	$RF_t \le 5$	25	7:30–18:30	1,525
Level 2	$5 < RF_t \le 10$	25	7:50–17:40	1,500
Level 3	$10 < RF_t \le 25$	33	7:40–17:40	2013
Level 4	$25 < RF_t \le 100$	24	6:50–17:40	1,584
Level 5	$100 < RF_t \le 300$	30	7:10–17:30	1890
Level 6	$RF_t > 300$	14	8:20–18:20	732

RF_t represents month rainfall. PAR_t represents photosynthetically active radiation.

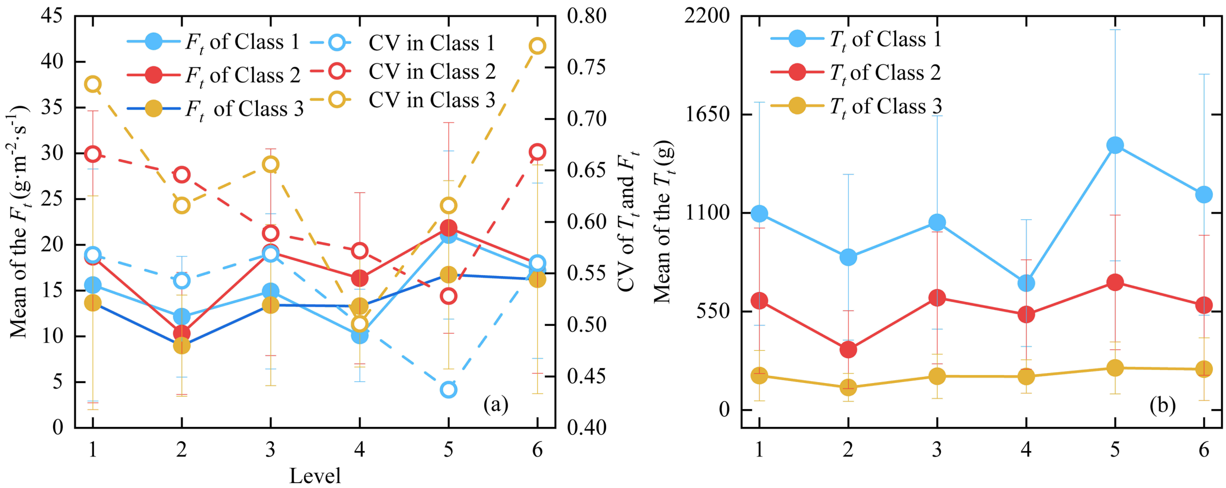

FIGURE 1
Changes in the original series of sap flux (Ft), daily transpiration (Tt) and their Coefficient of Variation (CV) across Levels 1 to 6. **(a)** mean values of Ft and CV for both Ft and Tt. **(b)** mean value of Tt.

T_t and F_t reached their highest values at Level 5, which may be attributed to their relative stability, indicated by lower CV value (Figure 1b).

Only the mean of SM_t varied consistently across the levels, indicating that monthly rainfall significantly affects SM_t. Compared to Level 1, SM_t showed a modest increase of 4% at Level 2, while it increased the most—by 52%—at Level 6 (Figure 2a). Additionally, SM_t exhibited the smallest variability among the factors (Figure 2b). For other environmental variables, the highest mean values of PAR_t, VPD_t and WS_t were observed at Level 5, Level 4 and Level 1, respectively, while the lowest values were found at Level 2 for PAR_t, Level 2 for VPD_t and Level 4 for WS_t (Figures 2a,b). Overall, WS_t exhibited the largest variability across Levels 1–4 (Figure 2b).

Model establishing and calibration

For rigor, the time series of all participating models used for training were stationary and no-white noise (Table 3). The first-order difference of SM_t (denoted as $D.\ SM_t$) for Level 2, 5 and 6 was stationary ($p < 0.05$), while $D.\ SM_t$ for Level 2 exhibited white noise characteristics ($p > 0.05$). The series for the others levels were stationary and non-white noise at the current order (p < 0.05).

Eighteen SVR models with linear kernels, based on Equation 8 and corresponding to six levels, were developed, with the predictions shown in Figure 3. Fifteen models across all three classes at Levels 1–5 were successfully constructed and performed very well based on Equations 6 and 7, with NSE values ranging from 0.77 ~ 0.98 and RSR values from 0.16 ~ 0.48. However, only three models corresponding to the three classes at level 6 performed poorly, with NSE values ranging from −0.41 to −0.17 and RSR values from 1.08 to 1.19.

Sensitivity of transpiration to environmental factors

From Figure 3f, the very poor performance of the SVM models at Level 6 indicated that the four environmental factors are insensitive to daily transpiration (T_t). As a result, the total contribution of all factors to T_t at Level 6 could not be predicted. At Levels 1–5, where high-accuracy prediction models were established, PAR_t was found to be the most sensitive factor to T_t, followed by VPD_t and WS_t, with SM_t exhibiting the least sensitivity (Figures 4d–f–8d–f). However, the sensitivity of the three classes did not differ significantly across Levels 1–5 ($p > 0.05$, Table 4), suggesting that the observed sensitivity is not related to tree size. Interestingly, the total contributions of PAR_t and VPD_t to T_t does not align with this order, except at levels 4 and 5 (Figures 4a–c–8a–c). The Mann–Whitney U test indicated that the contributions of all factors to T_t among the three classes did not differ significantly between Levels 1–5 ($p > 0.05$, Table 5). Similar results were observed within levels, except for WS_t at level 5 and SM_t at level 1. Additionally, the directions of contribution were consistent across the same levels. However, the effect of SM_t to T_t for three classes at Levels 2 and 5 could not be predicted, as $D.\ SM_t$ was considered white noise.

Interaction of environmental factors

External environmental factors not only affect the transpiration of trees individually but also regulate transpiration through complex interactions. For example, high PAR_t, and high VPD_t generally increase transpiration. However, under conditions of low SM_t or increased WS_t, trees may respond to these factors by closing their stomata, thereby limiting transpiration. The synergistic or antagonistic interactions among these factors depend on specific environmental conditions, plant species, and forest types. From Supplementary Figures 1, 4, 6, it is evident that SM_t (at Levels 1, 3 and 4), WS_t and VPD_t (at Levels 1–5) did not significantly impact the influence of PAR_t to T_t across the three tree classes at Levels 1, 3 and 4, as they transitioned without trends with PAR_t. This indicates that there is no interaction between SM_t and PAR_t, WS_t and PAR_t, or VPD_t and PAR_t concerning T_t. In contrast, SM_t negatively influenced the effects of VPD_t and the reduction of WS_t to the predicted T_t (Supplementary Figures 2, 3) across all classes at Levels 1, 3 and 4, except for class 1 at Level 1 (Supplementary Figures 2a$_1$, 3a$_1$).

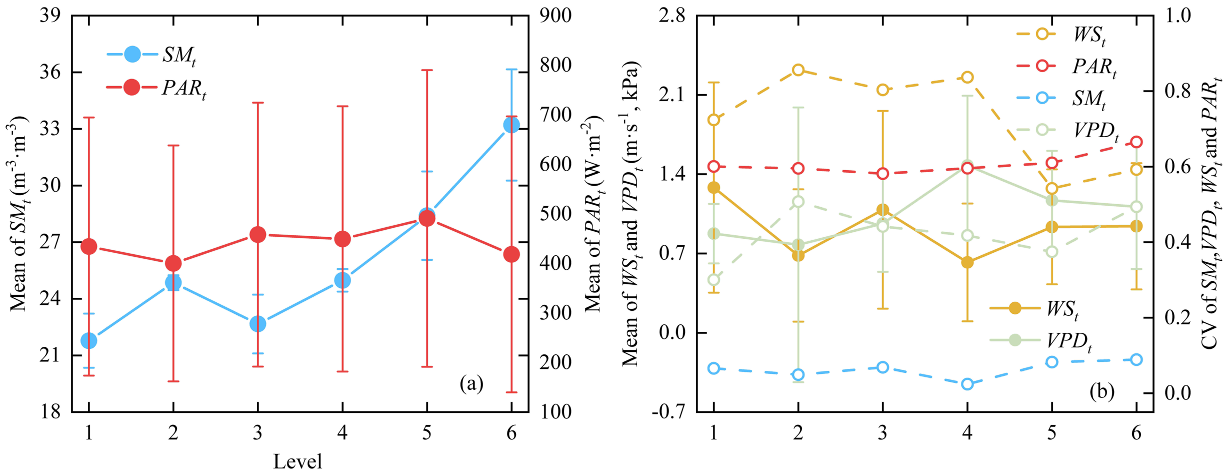

FIGURE 2
Changes in the original series of environmental factors and their Coefficient of Variation (CV) across Levels 1 to 6. **(a)** mean values of soil moisture (SMt) and photosynthetically active radiation (PARt). **(b)** mean values of wind speed (WSt), air vapor pressure deficit (VPDt), and the CV for SMt, VPDt and PARt.

Similarly, WS_t also negatively impacted the influence of VPD_t to T_t across all classes at Levels 1–5 (Supplementary Figure 5), except for Class 3 at Level 5 (Supplementary Figure 5e$_3$).

Discussion

Several key factors, including RF_t, Ta, RH, PAR_t, VPD_t, WS_t and SM_t, have been identified as major determinants of tree transpiration (e.g., Juhász et al., 2013; Shen et al., 2015; Wang et al., 2017; Wei et al., 2017; Xu and Yu, 2020; Chen et al., 2022). However, *Ta*, *RH*, and VPD_t, which is derived from the first two, are often considered simultaneously in regression models, potentially leading to collinearity issues (e.g., Yu et al., 2009; Liu et al., 2017; Wei et al., 2017; Han et al., 2019). While some studies employ principle component analysis (PCA) to address collinearity, eliminating multicollinear factors can enhance the efficiency of deep learning (DL) models (O'Brien et al., 2004; Juice et al., 2016; Xu and Yu, 2020; Li et al., 2022). Fan et al. (2020) compared the three ML models and one DL model in estimating daily maize transpiration, finding that deep neural networks (DNN) outperformed the others, with support vector machines (SVM) being the next best. In contrast, this study utilized an SVM that accounts for autocorrelation to analyze the sensitivity of the whole-tree transpiration of *S. superba* is to environmental factors, particularly because DNNs performed poorly. Variables included were PAR_t, VPD_t, WS_t and SM_t, while *Ta* and *RH* were excluded. Additionally, monthly precipitation was considered a limiting factor for measuring drought.

Overall, PAR_t and VPD_t exhibited the highest sensitivity to T_t when $RF_t \leq 300$ mm (Levels 1–5), during which the SVR models were well-developed. Numerous studies have been conducted across different climate zones and ecosystems. Based on traditional regression analysis, the influence of VPD_t on F_t and transpiration is often greater than that of PAR_t in tropical climate zones (e.g., Oguntunde and Oguntuase, 2007; Köhler et al., 2010; Huang et al., 2021). Conversely, in temperate climates, the impact of PAR_t tends to be greater than that of VPD_t (e.g., Huang et al., 2010; Yue et al., 2008; Zheng and Wang, 2015; Shen et al., 2015; Wei et al., 2017; Thomsen et al., 2020). Although this research was conducted in a subtropical climate zone, T_t was found to be more responsive to PAR_t than to VPD_t, aligning with the findings of Wang et al. (2017). However, VPD_t exhibited the opposite trend, except at Level 3, indicating that depressed trees are unable to tolerate water deficits in their leaves. This may be attributed to their relatively unstable CO_2 assimilation and low biomass allocation due to shallow roots (Sabir et al., 2020; Zafar et al., 2019). The effects of WS_t on F_t and transpiration were inconsistent due to substantial temporal variation (e.g., Tang et al., 2006; Chen et al., 2019; Chen et al., 2022), although significant effects were noted (e.g., Oguntunde and Oguntuase, 2007; Huang et al., 2010; Huang et al., 2015). There are primarily two different responses of transpiration to increases in WS_t, as noted by Laplace et al. (2013): linear responses (e.g., Juhász et al., 2013; Wang et al., 2017) and saturated responses (e.g., Li et al., 2022; Chen et al., 2024). Moreover, WS_t tends to affect the daytime F_t more than nighttime F_t (Han et al., 2019). In our study, WS_t was the third most sensitive factor affecting daytime T_t of *S. superba*, exhibiting linear decreases. Additionally, it influences other factors. Komatsu et al. (2006) found that the promotion of VPD_t to F_t depends on WS_t <0.7 m·s^{-1}. We observed that WS_t negatively influenced the overall promotion of VPD_t to T_t (Supplementary Figure 5). However, tree size did not significantly influence the responses of T_t to PAR_t, VPD_t and WS_t (Table 4), despite the theoretical expectation that larger trees would have a greater impact due to their increased surface area in contact with the atmosphere. The discrepancy may be attributed to variations in the actual contact area, which could depend on other factors such as the vertical distribution of leaf area and transient differences caused by fluctuations in wind speed, rather than just plant height and leaf size. Similar to WS_t, most studies suggest that SM_t significantly affects SF_t and transpiration, except for those by Tang et al. (2006), Shen et al. (2015), and Ma et al. (2017). Our results supports the views although it showed the least sensitive to T_t, which aligns with Huang et al. (2021). The finding that SM_t has a greater negative effect on T_t in Class 1 compared to the positive effects observed in Class 2 and 3 at the same level (level 4) is inconsistent with the observation that larger trees with deeper roots are less sensitive to depletion in SM_t

TABLE 3 Augmented Dickey-Fuller test for unit root and Portmanteau test for white noise.

Conditions	Test object	Lag length	Number of observations	5% Critical value	Test statistic	p-value	Portmanteau (Q) statistic	p-value
Level 1	T_t of Class 1	22	1,220	−3.410	−8.621	0.000	8756.050	0.000
	T_t of Class 2			−3.410	−8.644	0.000	9061.838	0.000
	T_t of Class 3			−3.410	−8.086	0.000	9337.683	0.000
	PAR_t			−3.410	−9.739	0.000	8856.676	0.000
	VPD_t			−1.950	−5.343	0.000	10274.288	0.000
	WS_t			−1.950	−2.941	0.000	15229.976	0.000
	SM_t			−2.860	−3.646	0.005	25651.070	0.000
Level 2	T_t of Class 1	22	1,200	−1.950	−10.554	0.000	8120.585	0.000
	T_t of Class 2			−1.950	−10.299	0.000	8919.100	0.000
	T_t of Class 3			−1.950	−9.953	0.000	9052.521	0.000
	PAR_t			−1.950	−10.333	0.000	8565.602	0.000
	VPD_t			−3.410	−7.463	0.000	8577.785	0.000
	WS_t			−1.950	−4.530	0.000	7688.037	0.000
	$D.SM_t$			−3.410	−7.577	0.000	7.287	0.999
Level 3	T_t of Class 1	24	1,647	−3.410	−10.622	0.000	12703.216	0.000
	T_t of Class 2			−3.410	−11.015	0.000	12770.674	0.000
	T_t of Class 3			−3.410	−8.682	0.000	13455.599	0.000
	PAR_t			−1.950	−11.534	0.000	13607.849	0.000
	VPD_t			−3.410	−7.492	0.000	12556.748	0.000
	WS_t			−1.950	−4.143	0.000	18216.559	0.000
	SM_t			−1.950	−2.510	0.000	33158.676	0.000
Level 4	T_t of Class 1	22	1,254	−3.410	−9.752	0.000	8409.517	0.000
	T_t of Class 2			−3.410	−9.877	0.000	9178.319	0.000
	T_t of Class 3			−1.950	−9.580	0.000	8645.546	0.000
	PAR_t			−3.410	−10.731	0.000	9022.630	0.000
	VPD_t			−3.410	−8.204	0.000	6832.120	0.000
	WS_t			−1.950	−4.002	0.000	8959.233	0.000
	SM_t			−2.860	−4.840	0.000	25952.219	0.000
Level 5	T_t of Class 1	23	1,512	−1.950	−9.329	0.000	9868.117	0.000
	T_t of Class 2			−1.950	−9.477	0.000	10321.484	0.000
	T_t of Class 3			−1.950	−9.232	0.000	11529.843	0.000
	PAR_t			−3.410	−10.438	0.000	9713.968	0.000
	VPD_t			−1.950	−5.148	0.000	14088.944	0.000
	WS_t			−3.410	−5.033	0.0002	7370.889	0.000
	$D.SM_t$			−1.950	−7.751	0.000	4.3486	1.000
Level 6	T_t of Class 1	18	610	−1.950	−4.678	0.000	4913.821	0.000
	T_t of Class 2			−1.950	−5.088	0.000	4961.036	0.000
	T_t of Class 3			−1.950	−5.412	0.000	5098.185	0.000
	PAR_t			−1.950	−4.566	0.000	3155.029	0.000
	VPD_t			−1.950	−2.720	0.000	6292.988	0.000
	WS_t			−1.950	−3.935	0.000	1626.305	0.000
	$D.SM_t$			−1.950	−5.641	0.000	32.735	0.018

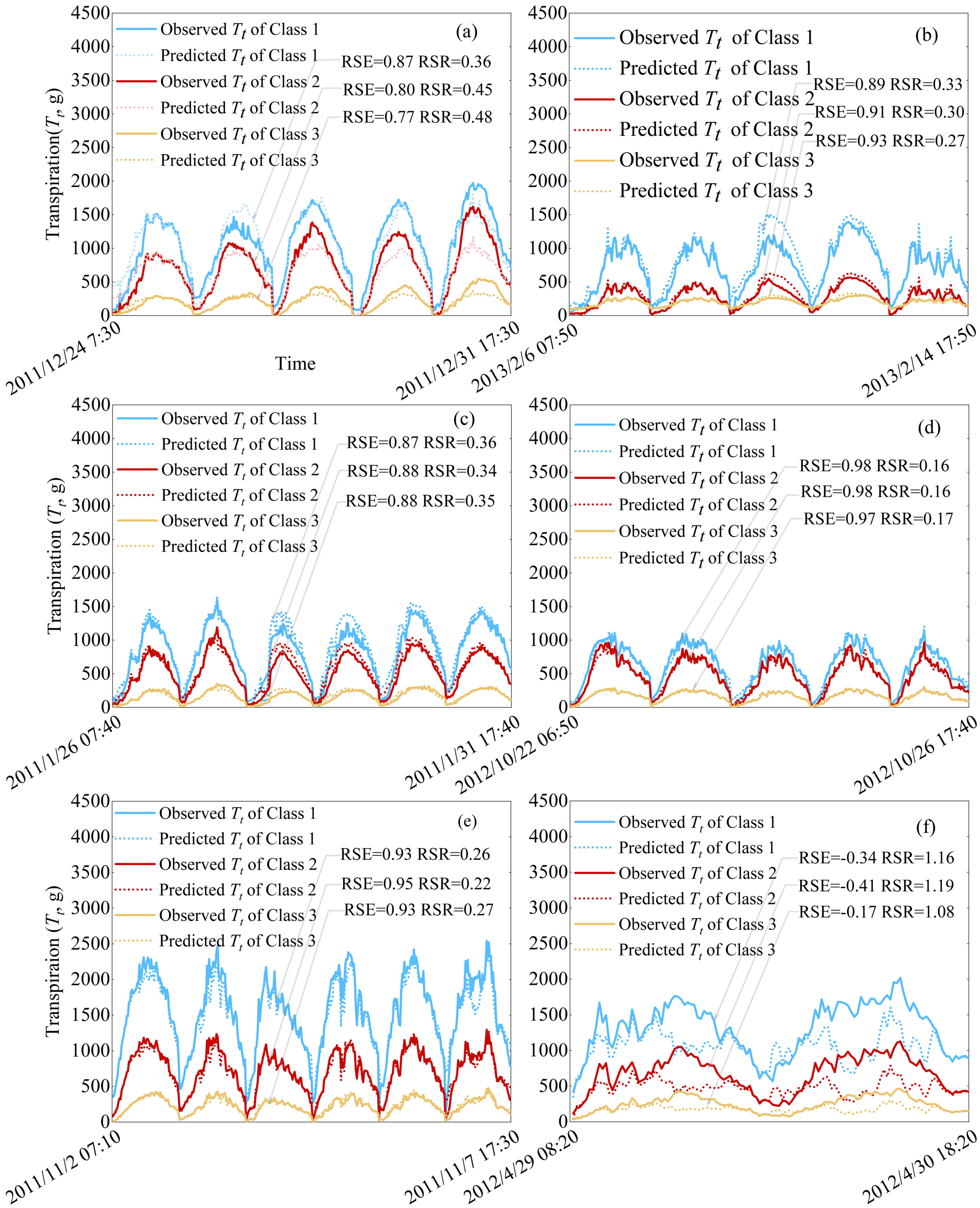

FIGURE 3
SVR testing results for daily transpiration in Classes1 to 3 across Levels 1 to 6. **(a)** Level 1. **(b)** Level 2. **(c)** Level 3. **(d)** Level 4. **(e)** Level 5. **(f)** Level 6.

(Dawson, 1996). This inconsistency may arise because trees benefit from more effective roots in the upper moist soil layer (Wei et al., 2017; Ochoa and Abdallah, 2023). Additionally, SM_t influenced the promotion of VPD_t and the demotion of WS_t in relation to T_t (Supplementary Figures 3, 5). However, it has no effect on the increase of PAR_t to T_t, nor do WS_t, VPD_t (Supplementary Figures 1, 4, 6), even during Level 1 of the worst drought. In other words, PAR_t affected T_t independently, while the others did not. Across different levels (1–5), the total contributions of all four factors to T_t also do not vary with tree size (Table 5). One

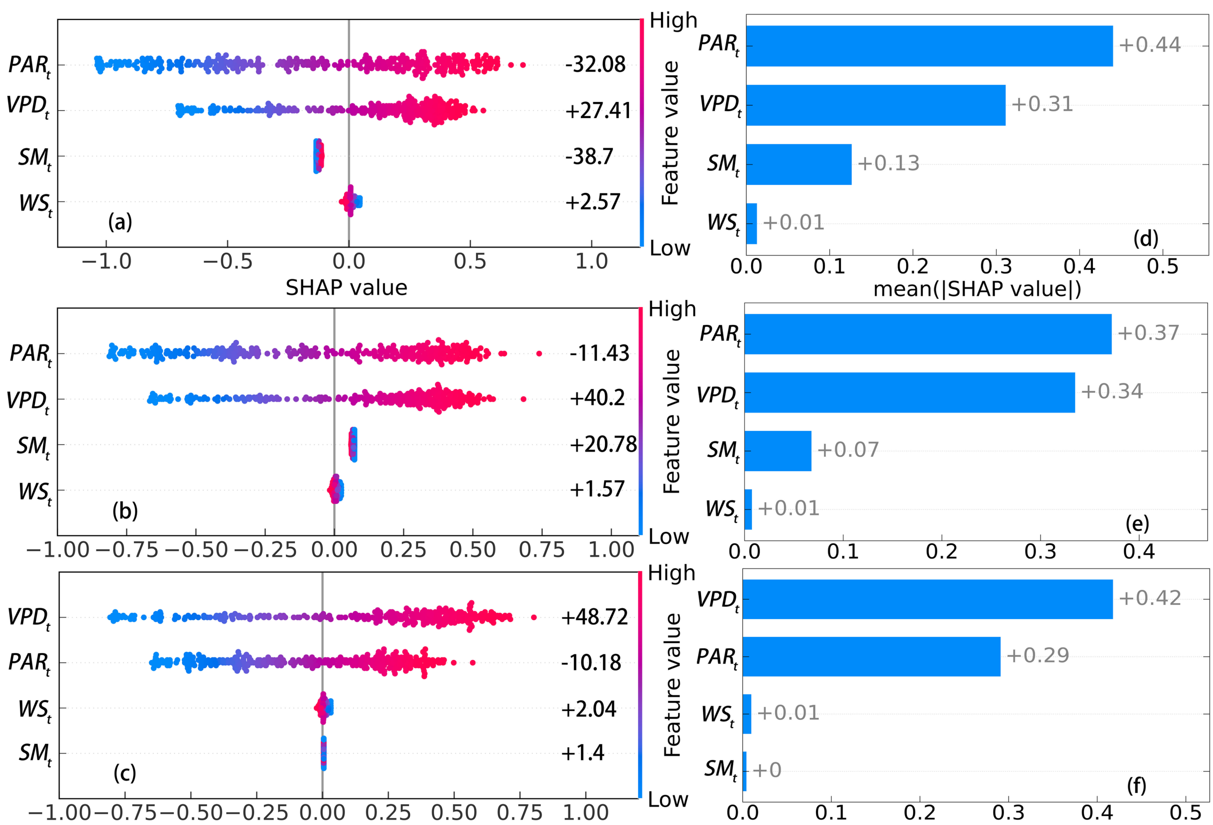

FIGURE 4
SHAP values of environmental factors affecting transpiration in Classes 1 to 3 at Level 1. **(a-c)** SHAP values for Class 1 to 3. **(d-f)** mean |SHAP values| for Class 1 to 3.

TABLE 4 Mann–Whitney *U* test results for the mean |SHAP| values of all factors across three classes at Level 1–5.

Factors	Group	Classes	Obs	Rank sum	Expected	*Z*-value	*p*-value
PAR_t VPD_t WS_t SM_t	Group 1	1	18	342	333	0.285	0.776
		2	18	324	333		
	Group 2	1	18	346	333	0.412	0.681
		3	18	320	333		
	Group 3	2	18	336	333	0.095	0.924
		3	18	330	333		

TABLE 5 Mann–Whitney U test for the accumulated SHAP values of all factors across three classes at Level 1–5.

Factors	Group	Classes	Obs	Rank sum	Expected	*Z*-value	*p*-value
PAR_t VPD_t WS_t SM_t	Group 1	1	18	316	333	−0.538	0.591
		2	18	350	333		
	Group 2	1	18	325	333	−0.253	0.800
		3	18	341	333		
	Group 3	2	18	340	333	0.221	0.825
		3	18	326	333		

possible cause could be that the drought was not severe enough, as our study site is located in a humid region of China. In contrast, a decoupling occurs between T_t and environmental factors when RF_t exceeds 300 mm. This decoupling may lead to an abnormal transpiration rate, resulting in the formation and accumulation of bubbles in the xylem ducts, which affects water transport and can cause cavitation in the xylem. Consequently, even during high rainfall months, if a tree has previously experienced drought stress, its

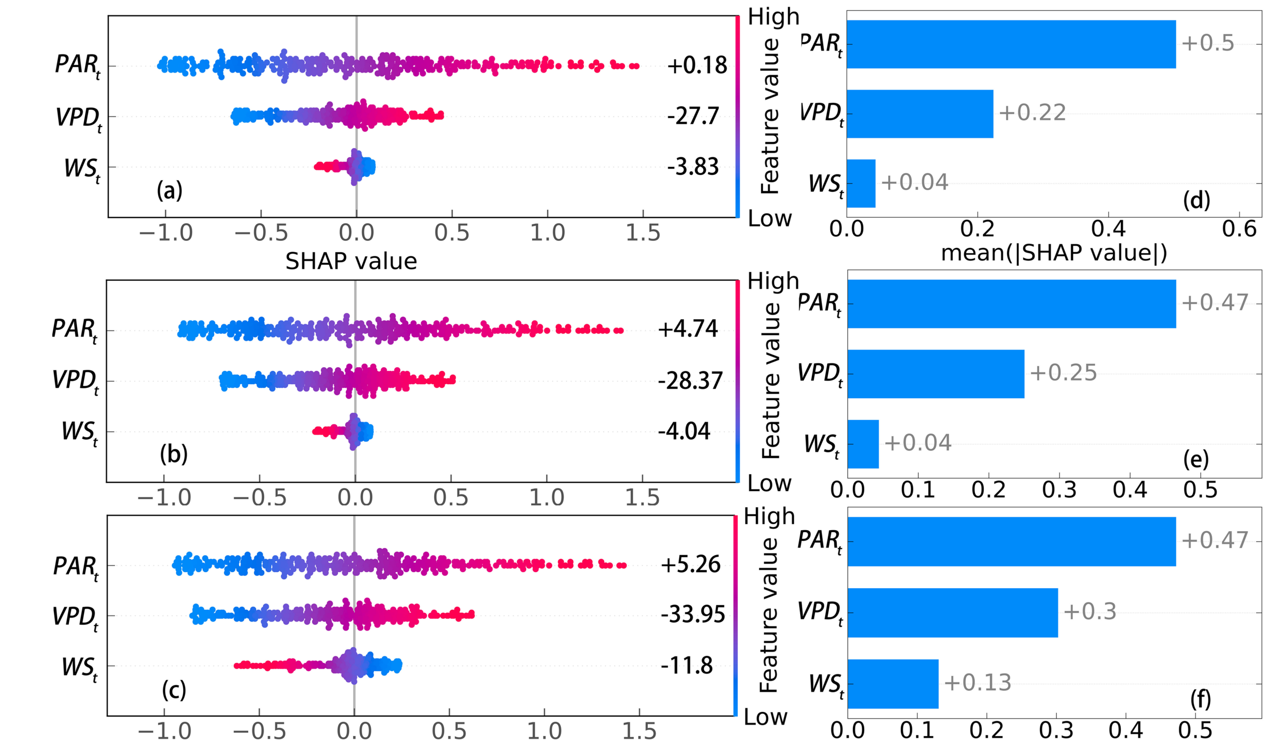

FIGURE 5
SHAP values of environmental factors affecting transpiration in Classes 1 to 3 at Level 2. **(a-c)** SHAP values for Class 1 to 3. **(d-f)** mean |SHAP values| for Class 1 to 3.

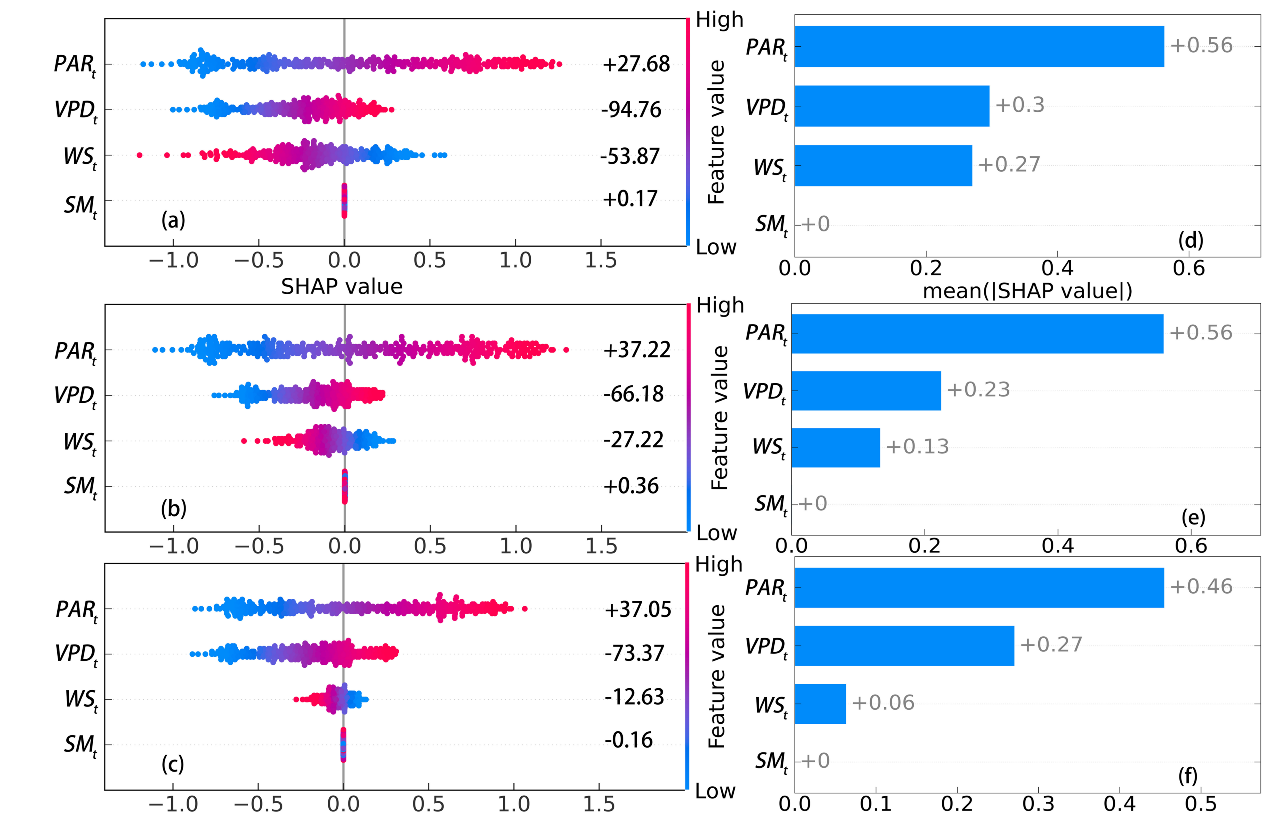

FIGURE 6
SHAP values of environmental factors affecting transpiration in Classes 1 to 3 at Level 3. **(a-c)** SHAP values for Class 1 to 3. **(d-f)** mean |SHAP values| for Class 1 to 3.

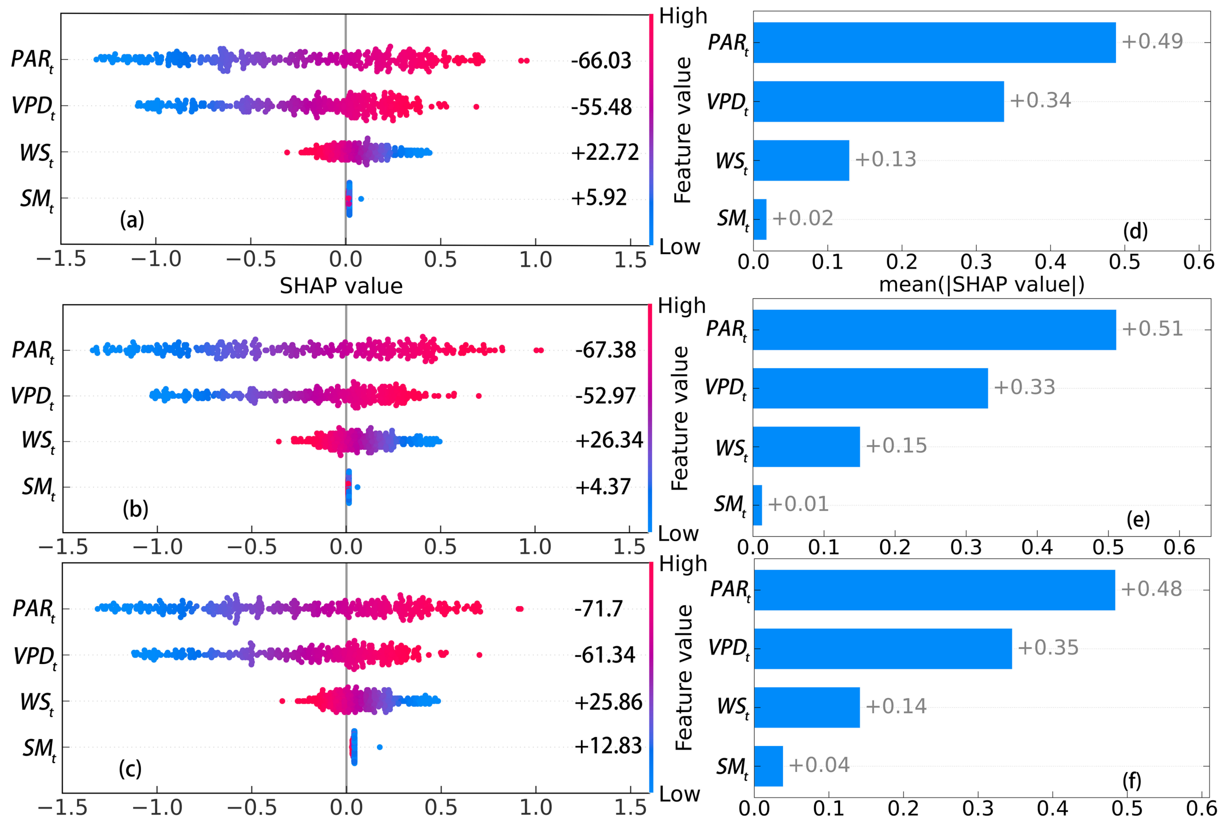

FIGURE 7
SHAP values of environmental factors affecting transpiration in Classes 1 to 3 at Level 4. **(a-c)** SHAP values for Class 1 to 3. **(d-f)** mean |SHAP values| for Class 1 to 3.

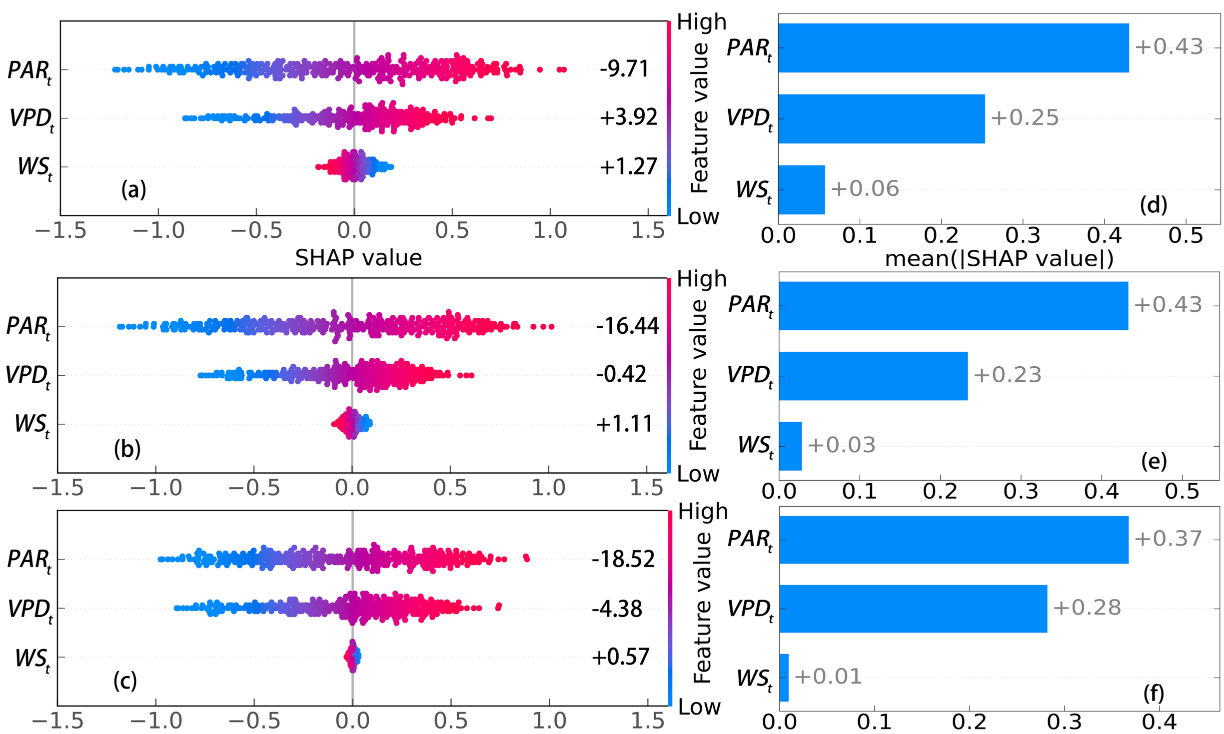

FIGURE 8
SHAP values of environmental factors affecting transpiration in Classes1 to 3 at Level 5. **(a-c)** SHAP values for Class 1 to 3. **(d-f)** mean |SHAP values| for Class 1 to 3.

transpiration rate may remain abnormal, leading to continued water stress. Additionally, some studies indicate that this abnormality is significantly related to the obstruction of stomatal behavior caused by rainfall (Smith and McClean, 1989; Meinzer et al., 1995; Meinzer et al., 1997; Lu et al., 2016). Therefore, it is essential to pay closer attention to the impact of immediate rainfall on transpiration and its relationship with environmental factors. Given the low sensitivity of SM_t on T_t in *S. superba*, we recommend mitigating the transpiration rate imbalance caused by rainfall thresholds by incorporating other shallow-rooted tree species.

Conclusion

This study demonstrates the application of Machine Learning (ML) in assessing tree water use concerning drought sensitivity analysis, revealing the threshold effect of monthly rainfall on the coupling of environmental factors in relation to transpiration. Five SVR models, which accounted for autocorrelation in daily transpiration of *S. superba* at five drought levels, revealed that daily transpiration is sensitive to all four environmental factors when $RF_t \leq 300$ mm, in the following order: $PAR_t > VPD_t > WS_t > SM_t$. The mean total contributions to T_t were ranked as follows: $VPD_t > PAR_t > WS_t > SM_t$. Additionally, this sensitivity and total contributions did not vary with tree size. However, when $RF_t > 300$ mm, daily transpiration becomes insensitive to all environmental factors.

Data availability statement

The data analyzed in this study is subject to the following licenses/restrictions: The data that support the findings of this study are available on request from the corresponding author. Requests to access these datasets should be directed to Xiaowei Zhao, xwzever@163.com.

Author contributions

XZ: Conceptualization, Formal analysis, Funding acquisition, Investigation, Methodology, Writing – original draft, Writing – review & editing. LZ: Data curation, Investigation, Project administration, Resources, Supervision, Writing – review & editing.

Funding

The author(s) declare that financial support was received for the research and/or publication of this article. This study was financially supported by the scientific Research Foundation for Ph.D, Shangluo University (23SKY010).

Conflict of interest

The authors declare that the research was conducted in the absence of any commercial or financial relationships that could be construed as a potential conflict of interest.

Generative AI statement

The authors declare that no Gen AI was used in the creation of this manuscript.

Publisher's note

Supplementary material

The Supplementary material for this article can be found online at: https://www.frontiersin.org/articles/10.3389/ffgc.2025.1572414/full#supplementary-material

References

Anderegg, W., Kane, J., and Anderegg, L. (2013). Consequences of widespread tree mortality triggered by drought and temperature stress. *Nat. Clim. Chang.* 3, 30–36. doi: 10.1038/nclimate1635

Andrade, J. L., Meinzer, F. C., Goldstein, G., Holbrook, N. M., Cavelier, J., Jackson, P., et al. (1998). Regulation of water flux through trunks, branches, and leaves in trees of a lowland tropical forest. *Oecologia* 115, 463–471. doi: 10.1007/s004420050542

Brunet, J., Inouye, D. W., Rankin, E. E. W., and Giannini, T. C. (2024). Global change aggravates drought, with consequences for plant reproduction. *Ann. Bot.* 135, 89–104. doi: 10.1093/aob/mcae186

Carvalho, D. R. A., Torre, S., Kraniotis, D., Almeida, D. P. F., Heuvelink, E., and Carvalho, S. M. P. (2015). Elevated air movement enhances stomatal sensitivity to abscisic acid in leaves developed at high relative air humidity. *Front. Plant Sci.* 6:383. doi: 10.3389/fpls.2015.00383

Chen, S. N., Chen, Z. S. N., Xu, H., Kong, Z., Xu, Z. B., Liu, Q. Q., et al. (2022). Biophysical regulations of transpiration and water use strategy in a mature Chinese pine (Pinus tabulaeformis) forest in a semiarid urban environment. *Hydrol. Process.* 36:e14485. doi: 10.1002/hyp.14485

Chen, L., Huang, J. G., Dawson, A., Zhai, L., Stadt, K. J., Comeau, P. G., et al. (2018). Contributions of insects and droughts to growth decline of trembling aspen mixed boreal forest of western Canada. *Glob. Chang. Biol.* 24, 655–667. doi: 10.1111/gcb.13855

Chen, S. N., Wei, W., and Huang, Y. (2024). Biophysical controls on canopy transpiration of Pinus tabulaeformis under different soil moisture conditions in the loess plateau of China. *J. Hydrol.* 631:130799. doi: 10.1016/j.jhydrol.2024.130799

Chen, X., Zhao, P., Hu, Y., Ouyang, L., Zhu, L., and Ni, G. (2019). Canopy transpiration and its cooling effect of three urban tree species in a sub-tropical city-Guangzhou, China. *Urban For. Urban Gree.* 43:126368. doi: 10.1016/j.ufug.2019.126368

da Silva, E. C., Albuquerque, M. B., Neto, A. D., and Junior, C. D. (2013). "Drought and its consequences to plants–from individual to ecosystem" in Responses of organisms to water stress. ed. S. Akinci (Rijeka, HR: INTECH d.o.o), 18–37.

Dawson, T. E. (1996). Determining water use by trees and forests from isotopic, energy balance and transpiration analyses: the roles of tree size and hydraulic lift. *Tree Physiol.* 16, 263–272. doi: 10.1093/treephys/16.1-2.263

Fan, J., Zheng, J., Wu, L., and Zhang, F. (2020). Estimation of daily maize transpiration using support vector machines; extreme gradient boosting; artificial and deep neural networks models. *Agr. Water Manage.* 245:106547. doi: 10.1016/j.agwat.2020.106547

Fricke, W. (2017). Water transport and energy. *Plant Cell Environ.* 406, 977–994. doi: 10.1111/pce.12848

Granier, A. (1985). Une nouvelle methode pour la measure du flux de seve brute dans le tronc des arbres. *Ann. Forest Sci.* 42, 193–200. doi: 10.1051/forest:19850204

Granier, A. (1987). Evaluation of transpiration in a Douglas-fir stand by means of sap flow measurements. *Tree Physiol.* 3, 309–320. doi: 10.1093/treephys/3.4.309

Han, C., Chen, N., Zhang, C., Liu, Y., Khan, S., Lu, K., et al. (2019). Sap flow and responses to meteorological about the *Larix principis-rupprechtii* plantation in Gansu Xinlong mountain, northwestern China. *For. Ecol. Manag.* 451:117519. doi: 10.1016/j.foreco.2019.117519

Holwerda, F., Bruijnzeel, L. A., Scatena, F. N., Vugts, H. F., and Meesters, A. G. C. A. (2012). Wet canopy evaporation from a Puerto Rican lower montane rain forest: the importance of realistically estimated aerodynamic conductance. *J. Hydrol.* 414-415, 1–15. doi: 10.1016/j.jhydrol.2011.07.033

Huang, K., Wang, Q., and Otieno, D. (2021). Responses of sap flux densities of different plant functional types to environmental variables are similar in both dry and wet seasons in a subtropical mixed Forest. *Forests* 12:1007. doi: 10.3390/f12081007

Huang, L., Zhang, Z. S., and Li, X. R. (2010). Sap flow of *Artemisia ordosica* and the influence of environmental factors in a revegetated desert area: Tengger Desert. *China. Hydrol. Process* 24, 1248–1253. doi: 10.1002/hyp.7584

Huang, J., Zhou, Y., Yin, L., Wenninger, J., Zhang, J., Hou, G., et al. (2015). Climatic controls on sap flow dynamics and used water sources of Salix psammophila in a semi-arid environment innorthwest China. *Environ. Earth Sci.* 73, 289–301. doi: 10.1007/s12665-014-3505-1

Jarvis, P. G. (1976). The interpretation of the variations in leaf water potential and stomatal conductance found in canopies in the field. *Philos Trans. R. Soc. London B. Biol. Sci.* 273, 593–610. doi: 10.1098/rstb.1976.0035

Jiao, L., Lu, N., Fang, W. W., Li, Z. S., Wang, J., and Jin, Z. (2019). Determining the independent impact of soil water on forest: a case study of a black locust plantation in the loess plateau, China. *J. Hydrol.* 572, 671–681. doi: 10.1016/j.jhydrol.2019.03.045

Juhász, Á., Sepsi, P., Nagy, Z., Tőkei, L., and Hrotkó, K. (2013). Water consumption of sweet cherry trees estimated by sap flow measurement. *Sci. Hortic.-Amsterdam* 164, 41–49. doi: 10.1016/j.scienta.2013.08.022

Juice, S. M., Templer, P. H., Phillips, N. G., Ellison, A. M., and Pelini, S. L. (2016). Ecosystem warming increases sap flow rates of northern red oak trees. *Ecosphere* 7:e01221. doi: 10.1002/ecs2.1221

Köhler, M., Schwendenmann, L., and Hölscher, D. (2010). Throughfall reduction in a cacao agroforest: tree water use and soil water budgeting. *Agric. For. Meteorol.* 150, 1079–1089. doi: 10.1016/j.agrformet.2010.04.005

Komatsu, H., Kang, Y., Kume, T., Yoshifuji, N., and Hotta, N. (2006). Transpiration from a Cryptomeria japonica plantation, part 2: responses of canopy conductance to meteorological factors. *Hydrological Processes*, 20, 1321–1334. doi: 10.1002/hyp.6094

Kono, Y., Ishida, A., Saiki, S. T., Yoshimura, K., Dannoura, M., Yazaki, K., et al. (2019). Initial hydraulic failure followed by late-stage carbon starvation leads to drought-induced death in the tree *Trema orientalis*. *Commun. Biol.* 2:8. doi: 10.1038/s42003-018-0256-7

Kume, A. (2017). Importance of the green color, absorption gradient, and spectral absorption of chloroplasts for the radiative energy balance of leaves. *J. Plant Res.* 130, 501–514. doi: 10.1007/s10265-017-0910-z

Laplace, S., Kume, T., Komatsu, H., and Chu, C.-R. (2013). Wind speed response of sap flow in five subtropical trees based on wind tunnel experiments. *BJECC* 3, 160–171. doi: 10.9734/BJECC/2013/3842

Li, S., Fang, L., Hegelund, J. N., and Liu, F. (2021). Elevated CO(2) modulates plant hydraulic conductance through regulation of PIPs under progressive soil drying in tomato plants. *Front. Plant Sci.* 12:666066. doi: 10.3389/fpls.2021.666066

Li, Y., Ye, J., Xu, D., Zhou, G., and Feng, H. (2022). Prediction of sap flow with historical environmental factors based on deep learning technology. *Comput. Electron. Agr.* 202:107400. doi: 10.1016/j.compag.2022.107400

Liu, X. Z., Kang, S. Z., and Li, F. S. (2009). Simulation of artificial neural network model for trunk sap flow of Pyrus pyrifolia and its comparison with multiple-linear regression. *Agr. Water Manage.* 96, 939–945. doi: 10.1016/j.agwat.2009.01.003

Liu, X., Zhang, B., Zhuang, J., Han, C., Zhai, L., Zhao, W., et al. (2017). The relationship between sap flow density and environmental factors in the Yangtze River Delta region of China. *Forests* 8:74. doi: 10.3390/f8030074

Lu, Y., Duursma, R. A., and Medlyn, B. E. (2016). Optimal stomatal behaviour under stochastic rainfall. *J. Theor. Biol.* 394, 160–171. doi: 10.1016/j.jtbi.2016.01.003

Ma, C., Luo, Y., Shao, M., Li, X., Sun, L., and Jia, X. (2017). Environmental controls on sap flow in black locust forest in loess plateau, China. *Sci. Rep.* 7:13160. doi: 10.1038/s41598-017-13532-8

Mastropietro, A., Feldmann, C., and Bajorath, J. (2023). Calculation of exact Shapley values for explaining support vector machine models using the radial basis function kernel. *Sci. Rep.* 13:19561. doi: 10.1038/s41598-023-46930-2

McDowell, N., Pockman, W. T., Allen, C. D., Breshears, D. D., Cobb, N., Kolb, T., et al. (2008). Mechanisms of plant survival and mortality during drought: why do some plants survive while others succumb to drought? *New Phytol.* 178, 719–739. doi: 10.1111/j.1469-8137.2008.02436.x

Mei, T. T., Wang, C. K., Zhao, P., Cai, X. A., Liu, X. J., Zhu, L. W., et al. (2010a). Dynamics of trunk sap flux density of *Schima superba*. *Scientia Silvae Sinicae* 46, 41–47. (in Chinese). doi: 10.11707/j.1001-7488.20100107

Mei, T. T., Zhao, P., Wang, Q., Cai, X. A., Yu, M. H., Zhu, L. W., et al. (2010b). Effects of tree diameter at breast height and soil moisture on transpiration of *Schima superba*. *Chin. J. Appl. Ecol.* 21, 2457–2464. (in Chinese). doi: 10.3724/SP.J.1231.2010.06753

Meinzer, F. C. (2003). Functional convergence in plant response to the environment. *Oecologia* 134, 1–11. doi: 10.1007/s00442-002-1088-0

Meinzer, F. C., Andrade, J. L., Goldstein, G., Holbrook, N. M., Cavelier, J., and Jackson, P. (1997). Control of transpiration from the upper canopy of a tropical forest: the role of stomatal, boundary layer and hydraulic architecture components. *Plant Cell Environ.* 20, 1242–1252. doi: 10.1046/j.1365-3040.1997.d01-26.x

Meinzer, F. C., Goldstein, G., and Andrade, J. L. (2001). Regulation of water flux through tropical forest canopy trees: do universal rules apply? *Tree Physiol.* 21, 19–26. doi: 10.1093/treephys/21.1.19

Meinzer, F. C., Goldstein, G., Jackson, P., Holbrook, N. M., Gutiérrez, M. V., and Cavelier, J. (1995). Environmental and physiological regulation of transpiration in tropical forest gap species: the influence of boundary layer and hydraulic properties. *Oecologia* 101, 514–522. doi: 10.1007/BF00329432

Monteith, J., and Mike, H. (1990). Principles of environmental physics. London: Edward Asner publishers.

Moriasi, D., Arnold, J., Van Liew, M., Bingner, R., Harmel, R., and Veith, T. (2007). Model evaluation guidelines for systematic quantification of accuracy in watershed simulations. *Int. J. Agr. Biol. Eng.* 50, 885–900. doi: 10.13031/2013.23153

O'Brien, J. J., Oberbauer, S. F., and Clark, D. B. (2004). Whole tree xylem sap flow responses to multiple environmental variables in a wet tropical forest. *Plant Cell Environ.* 27, 551–567. doi: 10.1111/j.1365-3040.2003.01160.x

Ochoa, C. G., and Abdallah, M. A. B. (2023). The seasonal variability and environmental factors influencing the transpiration of Western Juniper (*Juniperus occidentalis*) saplings. *Hydro.* 10:232. doi: 10.3390/hydrology10120232

Oguntunde, P. G., and Oguntuase, A. M. (2007). Influence of environmental factors on the sap flux density of mango trees under rain-fed cropping systems in West Africa. *Int. J. Plant Prod.* 1, 179–188. doi: 10.22069/ijpp.2012.535

Sabir, M. A., Rasheed, F., Zafar, Z., Khan, I., Nawaz, M. F., Ul Haq, I., et al. (2020). A consistent CO_2 assimilation rate and an enhanced root development drives the tolerance mechanism in *Ziziphus jujuba* under soil water deficit. *Arid Land Res. Manag.* 34, 392–404. doi: 10.1080/15324982.2020.1748140

Saha, S., Kundu, B., Paul, G. C., and Pradhan, B. (2023). Proposing an ensemble machine learning based drought vulnerability index using M5P, dagging, random sub-space and rotation forest models. *Stoch Environ Res Risk Assess* 37, 2513–2540. doi: 10.1007/s00477-023-02403-6

Shen, Q., Gao, G., Fu, B., and Lü, Y. (2015). Sap flow and water use sources of shelter-belt trees in an arid inland river basin of Northwest China. *Ecohydrology* 8, 1446–1458. doi: 10.1002/eco.1593

Smith, W. K., and McClean, T. M. (1989). Adaptive relationship between leaf water repellency, stomatal distribution, and gas exchange. *Am. J. Bot.* 76, 465–469. doi: 10.1002/j.1537-2197.1989.tb11335.x

Smola, A. J., and Schölkopf, B. (2004). A tutorial on support vector regression. *Stat. Comput.* 14, 199–222. doi: 10.1023/B:STCO.0000035301.49549.88

Tang, J., Bolstad, P. V., Ewers, B. E., Desai, A. R., Davis, K. J., and Carey, E. V. (2006). Sap flux–upscaled canopy transpiration, stomatal conductance, and water use efficiency in an old growth forest in the Great Lakes region of the United States. *J. Geophys. Res. Biogeosci.* 111, 1–12. doi: 10.1029/2005JG000083

Thomsen, S., Reisdorff, C., Gröngröft, A., Jensen, K., and Eschenbach, A. (2020). Responsiveness of mature oak trees (*Quercus robur* L.) to soil water dynamics and meteorological constraints in urban environments. *Urban Ecosyst.* 23, 173–186. doi: 10.1007/s11252-019-00908-z

Tu, J., Wei, X. H., Huang, B. B., Fan, H. B., Jian, M. F., and Li, W. (2019). Improvement of sap flow estimation by including phenological index and time-lag effect in back-propagation neural network models. *Agric. For. Meteorol.* 276-277:107608. doi: 10.1016/j.agrformet.2019.06.007

Uexkull, N., Croicu, M., Fjelde, H., and Buhaug, H. (2016). Civil conflict sensitivity to growing-season drought. *Proc. Natl. Acad. Sci. USA* 113, 12391–12396. doi: 10.1073/pnas.1607542113

Vapnik, V. N. (1995). The nature of statistical learning theory. New York: Springer Nature.

Wang, X., Liu, J., Sun, Y., Li, K., and Zhang, C. (2017). Sap flow characteristics of three afforestation species during the wet and dry seasons in a dry-hot valley in Southwest China. *J. For. Res.* 28, 51–62. doi: 10.1007/s11676-016-0276-4

Wei, X., Li, B., Guo, C., Wang, Y., He, J., Liu, S., et al. (2017). Identification of sap flow driving factors of jujube plantation in semi-arid areas in Northwest China. *Int. J. Agric. Biol. Eng.* 10, 172–183. doi: 10.3965/j.ijabe.20171002.2140

Whitley, R., Medlyn, B., Zeppel, M., Macinnis-Ng, C., and Eamus, D. (2009). Comparing the penman—Monteith equation and a modified Jarvis—Stewart model with an artificial neural network to estimate stand-scale transpiration and canopy conductance. *J. Hydrol.* 373, 256–266. doi: 10.1016/j.jhydrol.2009.04.036

Wullschleger, S. D., Meinzer, F. C., and Vertessy, R. A. (1998). A review of whole-plant water use studies in trees. *Tree Physiol.* 18, 499–512. doi: 10.1093/treephys/18.8-9.499

Xu, S. Q., and Yu, Z. B. (2020). Environmental control on transpiration: a case study of a desert ecosystem in Northwest China. *Water* 12:1211. doi: 10.3390/w12041211

Xu, S. Q., Yu, Z. B., Ji, X. B., and Sudicky, E. A. (2017). Comparing three models to estimate transpiration of desert shrubs. *J. Hydrol.* 550, 603–615. doi: 10.1016/j.jhydrol.2017.05.027

Yu, Z. H., Chen, Y. M., and Du, S. (2009). The sapflow dynamics of *Platycladus orientalis* in the semi-arid loess plateau region. *Acta Ecol. Sin.* 29, 3970–3976. (in Chinese). doi: 10.3321/j.issn:1000-0933.2009.07.061

Yue, G., Zhao, H., Zhang, T., Zhao, X., Li, N., and Drake, S. (2008). Evaluation of water use of *Caragana microphylla* with the stem heat-balance method in Horqin Sandy land, Inner Mongolia, China. *Agr. Forest Meteorol.* 148, 1668–1678. doi: 10.1016/j.agrformet.2008.05.019

Zafar, Z., Rasheed, F., Abdullah, M., Salam, M. M. A., and Mohsin, M. (2019). Effects of water deficit on growth and physiology of young *Conocarpus erectus* L. and *Ficus benjamina* L. saplings. *Bangladesh J. Bot.* 48, 1215–1221. doi: 10.3329/bjb.v48i4.49078

Zhang, Q., Han, L. Y., Lin, J. J., and Cheng, Q. Y. (2018). North–south differences in Chinese agricultural losses due to climate-change-influenced droughts. *Theor. Appl. Climatol.* 131, 719–732. doi: 10.1007/s00704-016-2000-x

Zhang, H., Loaiciga, H. A., and Sauter, T. A. (2024). Novel fusion-based methodology for drought forecasting. *Remote Sens.* 16:828. doi: 10.3390/rs16050828

Zhao, X. W., Ouyang, L., Zhao, P., and Zhang, C. F. (2018). Effects of size and microclimate on whole-tree water use and hydraulic regulation in Schima superba trees. *PeerJ* 6:e5164. doi: 10.7717/peerj.5164

Zheng, C., and Wang, Q. (2015). Seasonal and annual variation in transpiration of a dominant desert species, Haloxylon ammodendron, in Central Asia up-scaled from sap flow measurement. *Ecohydrology* 8, 948–960. doi: 10.1002/eco.1547

Zia, R., Nawaz, M. S., Siddique, M. J., Hakim, S., and Imran, A. (2021). Plant survival under drought stress: implications, adaptive responses, and integrated rhizosphere management strategy for stress mitigation. *Microbiol. Res.* 242:126626. doi: 10.1016/j.micres.2020.126626